Colloids and Surfaces B: Biointerfaces 149 (2017) 168–173

Contents lists available at ScienceDirect

Colloids and Surfaces B: Biointerfaces

journal homepage: www.elsevier.com/locate/colsurfb

Modulus-regulated 3D-cell proliferation in an injectable self-healing hydrogel

Yongsan Li[a,b], Yingwei Zhang[a], Feng Shi[a,*], Lei Tao[b,*], Yen Wei[b], Xing Wang[a,*]

[a] Beijing Laboratory of Biomedical Materials, Beijing University of Chemical Technology, Beijing 100029, PR China
[b] The Key Laboratory of Bioorganic Phosphorus Chemistry & Chemical Biology (Ministry of Education), Department of Chemistry, Tsinghua University, Beijing 100084, PR China

ARTICLE INFO

Article history:
Received 12 August 2016
Received in revised form 6 October 2016
Accepted 10 October 2016
Available online 12 October 2016

Keywords:
3D cell culture
Proliferation
Hydrogel
Mechanical-strength
Injection

ABSTRACT

Cell therapy has attracted wide attention among researchers in biomaterial and medical areas. As a carrier, hydrogels that could keep high viability of the embedded cells have been developed. However, few researches were conducted on 3D cell proliferation, a key factor for cell therapy, especially after injection. In this study, we demonstrated for the first time the proliferation regulation of the 3D-embedded L929 cells in a modulus-tunable and injectable self-healing hydrogel before and after injection without adding specific growth factor. The cells showed a stiffness-dependent proliferation to grow faster in higher stiffness hydrogels. The proliferating rates of the encapsulated cells before and after injection were quantified, and the shearing force as a possible negative influence factor was discussed, suggesting the both internal property of the hydrogel and injection process are critical for further practical applications. Due to the high operability and good biocompatibility, this injectable self-healing hydrogel can be a promising carrier for cell therapy.

1. Introduction

Cell therapy has been considered as the most direct approach to achieve the therapeutic purpose by replacing/restoring the physiological functions of damaged tissue or organs [1], and thus drawn great focus among researchers from both biological and clinical medical areas. Despite of the inevitable immune reactions and extremely low targeting compatibility, the direct infusion of functional cells, the first generation cell therapy method, has been employed in the clinic trial for decades to achieve many remarkable successes [2,3], indicating the huge potential of cell therapy.

To protect the transplanted cells from the attack of the immune system and improve the utilization efficiency, encapsulating cells in 3-dimensional (3D) carriers has been developed as the second generation cell therapy method [4–6]. Among various 3D cell carriers including polymer microcapsules, micro-gels, and bio-cements etc., injectable hydrogels demonstrate intrinsic superiority to facilely deliver and concentrate abundant cells to the desired positions while avoiding implanting surgery and potential re-surgery risk [7–10]. So far, different injectable hydrogels have been explored as the carriers for cell therapy [11,12], and the loadings as well as the viability of incubated cells before/after injection have been investigated [13–15]. However, there is still a big gap from bench to bedside for the application of those injectable hydrogels in clinical cell-therapy, the main limitations are: 1) Many injectable hydrogels are prepared depending on the change of physical conditions (physical hydrogels), such as some thermos-sensitive hydrogels. After injection, the gelation processes of those physical hydrogels are difficult to control [16,17]. Meanwhile, the drastic change of physical conditions (temperature, pH, etc.) might also affect the cell viability. 2) Some hydrogels are generated via covalent bonds through chemical reactions (chemical hydrogels). The complexity of the chemical reactions and the potential toxicity of those reagents/catalysts greatly restrict the further *in vivo* applications of those hydrogels [18–20]. 3) In most artificial polymer hydrogels, growth factors such as EGF or FGF have to be added to prompt the proliferation of the encapsulated cells, which might introduce some potential risks to the surrounding tissues [21,22]. Therefore, developing a gelation-controllable, biocompatible and biodegradable hydrogel in which the encapsulated cells can not only keep high viability but also proliferation without adding specific growth factor even after injection to realize their functions is of great importance for future cell-therapy (Scheme 1).

Our group developed an injectable, self-healing chitosan-based dynamic hydrogel (CP hydrogel) using the biocompatible glycol-

* Corresponding authors.
E-mail addresses: shi@mail.buct.edu.cn (F. Shi), leitao@mail.tsinghua.edu.cn (L. Tao), wangxing@mail.buct.edu.cn (X. Wang).

http://dx.doi.org/10.1016/j.colsurfb.2016.10.021
0927-7765/

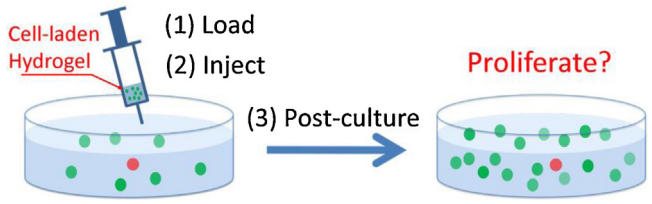

Scheme 1. Graphical representation of the injection procedure for mimicking the cell therapy process, and the proliferation of the survived cells evaluated within the post-culture experiment.

chitosan (GCS) and dibenzaldehyde-terminated poly(ethylene-glycol) (DF-PEG) as the gelators [23,24]. By simply mixing the two solutions of GCS and DF-PEG, the CP hydrogel could be prepared within 1 min. The CP hydrogel is constructed by dynamic Schiff-base that keeps breaking and regenerating in the hydrogel network [25–28], thus leading to the injectable and self-healing properties [29–31]. Different from other injectable hydrogels using liquid precursors prior to the injection, this interesting hydrogel could be crushed and pushed through a needle as solid hydrogel pieces, then recovered as a whole under physiological condition without external stimuli, avoiding the uncontrollable gelation process and the drastic change of physical conditions. As a result, cells can survive very well in that CP hydrogel even after injection. In our previous research, after extra-adding growth factors, that CP hydrogel could be used as a carrier for cell therapy to repair the damaged central nervous system in zebra fish [32].

Recently, Anseth et al. reported stem cells possess memory on past stiffness-different hydrogels' surfaces [33], inspiring us to use this 2D character into 3D application to develop a hydrogel carrier for cell therapy only by modulating mechanical factor. Encouraged by our previous research, we hope to upgrade the injectable CP hydrogel as a controllable culture environment for cell proliferation. Only by simply tuning the modulus through varying the ratio of the two gelators, an injectable hydrogel for cells direct or post culture and proliferation can be achieved. So far as we know, it is the first report about proliferation of the injected 3D-embedded cells in a self-healing hydrogel without extra added growth factor, suggesting the self-healing hydrogel a promising soft matter as the cell-therapy carrier.

2. Experiments

2.1. Materials

DF-PEG (Mn ~ 4000) was synthesized as our previous papers [23]. Glycol chitosan (Wako Pure Chemical Industries, 90% degree of deacetylation), RPMI-1640 culture medium, fetal bovine serum (FBS), penicillin-streptomycin solution (GE Healthcare), fluorescein diacetate and propidium iodide (FDA/PI, Invitrogen), were used as received.

2.2. Preparation of the hydrogels

A series of hydrogels were prepared followed the method below. Typically, glycol-chitosan (0.03 g) was firstly dissolved in deionized water (0.97 g), then, mixed with the same volume of solutions with 2 wt%, 4 wt% and 8 wt% DF-PEG solutions respectively, to form 3 different hydrogels with different moduli. As the control, a hydrogel with the same concentration of glycol-chitosan, 2 wt% DF-PEG and 2 wt% PEG (without aldehyde endings) was prepared by the same process.

2.3. Rheology analyses

2.3.1. Original hydrogels

The rheology analyses of the hydrogel were carried out to evaluate the moduli of the series of hydrogels. Typically, glycol chitosan solution (0.2 g, 3 wt%) was spread on a parallel plate. Then, DF-PEG aqueous solution (0.2 g, 2 wt%) was evenly added dropwise onto the chitosan solution surface and mixed with pipette quickly. The storage modulus (G') values versus frequency analyses were carried out using a steel plate (diameter: 20 mm) and performed at 1% strain and 6.3 rad s^{-1}

2.3.2. Self-healed hydrogels

A 400 μL of hydrogel was firstly prepared on the parallel plate. After complete gelation of the hydrogel, a time versus moduli figure was recorded as a reference. Then the test was paused and the hydrogel was cut into 25 pieces to mimic the damage of the hydrogel after injection while maintaining the contacting area between the hydrogel and the upper steel plate. Analysis was resumed to monitor the self-healing process of the damaged hydrogels. Subsequently, a frequency-dependent rheological test was also carried out to evaluate the modulus of the self-healed hydrogels.

2.4. Normal 3D cell encapsulation and proliferation

2.4.1. Cell culture

L929 cells were cultured in RPMI-1640 supplemented with 10% FBS, 5% penicillin-streptomycin and incubated at 37 °C, 5% CO_2. The medium was changed every day. The cells were harvested with PBS containing 0.025 (w/v) % trypsin and 0.01% EDTA, centrifuged and re-suspended in the RPMI-1640 medium.

2.4.2. Cell encapsulation

L929 cells were harvested and re-suspended in RP1640 media and diluted to reach 2.5×10^6 cells mL^{-1}. The diluted cell suspension was mixed with same volume of GCS culture media solution followed by triturating 15–20 times. The cell-chitosan suspension was pipetted to the central part of a petri-dish, and mixed with $DF\text{-}PEG_{4000}$ culture media solution with different concentration to form a series of hydrogels. All encapsulation studies were performed with 1.5×10^6 cells mL^{-1} in the series of gels. An addition amount of culture media was added on the top of the hydrogels after complete gelation to avoid the evaporation, provide nutrition and metabolite exchange of the embedded cells.

2.4.3. Cell proliferation

The cell-laden hydrogels were incubated at 37 °C, 5% CO_2, and imaged after encapsulating 3 days, 5 days and 7 days. The hydrogels were stained with FDA/PI and visualized by confocal microscopy to evaluate the cell viability and proliferation. Constructs were excited at 488 nm and 543 nm wavelengths to visualize live and dead cells, respectively, and z-stacks were taken through the depth of the gels to validate an even distribution of cells throughout.

2.4.4. Cell counting

After confocal imaging, the hydrogel was degraded with 1 mL of 3.0 wt% acetic acid solution. Subsequently, the acid containing cell suspension was centrifuged and the cells were re-suspended in 2 mL culture media. Then, the cell counting of each hydrogel was carried out 3 times, using a blood counting chamber as a routine.

2.5. Injection and proliferation

The cell-laden hydrogels were prepared with above-mentioned method (2.4.). The hydrogel was then loaded in a 48-gauge-needle syringe and injected to the petri-dish. After the denoted periods,

the confocal microscopy and cell counting analyses were carried out with the same way.

3. Results and discussion

3.1. Rheology analyses

3.1.1. Original hydrogels

A series of hydrogels with different moduli were prepared using the same wt% of GCS (1.5%) and different wt% of DF-PEG$_{4000}$ (1%, 2%, 4%). Rheology test was employed to evaluate the hydrogels (Fig. 1). The storage moduli (G') of those hydrogels were found approximately 0.9 kPa (1%, soft), 2.1 kPa (2%, medium) and 4.7 kPa (4%, stiff), respectively (Fig. 1A), which is contributed to the higher cross-linking density by adding more cross-linker in the hydrogel network, resulting in higher storage modulus (greater stiffness) [34–36]. Interestingly, we find the modulus of the stiff hydrogel near that of the subcutaneous tissue [37] (5.6 kPa, in vivo environment of L929 cells). So the stiff hydrogel might mimic the ECM best and providing highest cell proliferation rate.

It is well known that PEG could affect the cell condition and behaviours, the mass of the cross-linker DF-PEG might also be a factor to influence the cell proliferation. Therefore, a control experiment was designed to test this hypothesis. By using 2% DF-PEG (cross-linker) and 2% PEG (without active terminal), a control hydrogel was prepared. Although this hydrogel has PEG mass as equal as the hard hydrogel (4%), the storage modulus is similar to the medium hydrogel (~2.1 kPa Fig. 1A, gray).

3.1.2. Self-healed hydrogels

The CP hydrogel could self-heal after injection. To monitor the self-healing process, a rheology test was carried out to record the change of modulus according to increase time, and the results were shown in Fig. 1B. The storage modulus G' dropped sharply after damage, then increased with time (Fig. 1B) until reached similar level as the pristine hydrogel, illustrating the self-healing process. The soft hydrogel healed to its original modulus G' after 40 min, while the stiff one spent longer time (84 min) to heal itself. The middle and control groups displayed almost the same healing time (around 52 ~ 56 min), suggesting that adding PEG mass did not influence the modulus of this CP hydrogel. Finally, all the test hydrogels recovered from damaging to the storage modulus G' as same as the original ones (Fig. 1C).

3.2. Injection and proliferation

In cell therapy, implanting cells with injectable hydrogel has incomparable advantage over intravenous infusion to greatly enhance the delivery efficiency and viability of the implanted cells. To evaluate this injectable hydrogel as a carrier for cell therapy, an injection mimicking and following post-culturing experiment was carried out (Fig. 2). L929 cell, a typical fibroblast cell line, was used as a model cell to be embedded in above-mentioned hydrogels. Typically, glycol chitosan (GCS) was firstly dissolved in RPMI-1640 culture media, and mixed with L929 cell suspension to get cell containing GCS solution. The cell containing GCS solution was then mixed with DF-PEG solution to form cell-laden CP hydrogel.

As shown in Fig. 2A, the cell embedded hydrogel (solid) was loaded in a syringe and then squeezed out through a 48-guage needle into a Petri dish followed by a 7-day post-culturing process. The squished CP hydrogel pieces (Fig. 2A1) self-healed to reform an integrated hydrogel (Fig. 2A2) after injection, which is crucial for cell therapy.

To confirm the proliferation *in situ* after injection, the fissional process of cells in the CP hydrogel was checked and exhibited through both optical microscopy (Fig. 2B) and fluorescent microscopy (Fig. 2C, staining with FDA/PI reagents [38]) methods. Compared with the image taken just after encapsulation (Fig. 2B, 2C), the cell density increased dramatically within 7 days (Fig. 2B1, 2C1). In the enlarged vision, more detailed cell-fissional process could also be observed. Some cells are found to divide from one to two (pointed with red arrows), directly confirming the 3D cell proliferation in the CP hydrogel.

3.3. Proliferation before injection: influence of stiffness

Firstly, the influence of hydrogel stiffness (without injection) on the cell proliferation was studied. The L929 cell-contained GCS solution was mixed with different concentrated DF-PEG solutions to form cell-laden CP hydrogels with the same cell amount (1.5 million cells mL^{-1}) but different stiffness. The cell viability and the proliferating status in the 3D-hydrogels were recorded by the fluorescent confocal images (Fig. 3). It can be easily observed that cells in all of the hydrogels showed extremely high viability (>99%) throughout the culture process, confirming the excellent biocompatibility of the CP hydrogels. Meanwhile, the cell proliferation showed obvious stiffness-dependence. The cells have been encapsulated in each hydrogel with similar initial density, so the change of cell density during the observing process would reflect the proliferation rate. As shown in Fig. 3A, the cell density in the soft hydrogel showed unremarkable increase. On the contrary, the cell number obviously increased within the medium hydrogels (Fig. 3B), and arrived the maximum in the stiff hydrogel (Fig. 3C), preliminary suggesting the increased storage modulus prompted the L929 cells proliferation, even under growth factor free condition.

The proliferation of L929 cells in the control hydrogel (Fig. 3D) displayed similar cell density with the medium group (Fig. 3B), demonstrating the storage modulus rather than the PEG mass in hydrogel is the direct reason for cell proliferation. And these regulations were confirmed and would be discussed by the following statistical analyses.

3.4. Proliferation after injection: influence of shearing force

After injection, the shearing force really caused some cells' death, as visible red signal (PI staining) could be found in the images (Fig. 3A'–D'). But the remained living cells also showed stiffness-dependence proliferation. The cell density increased faster in the stiff hydrogel than in the medium and soft hydrogels, similar with the phenomena in the original hydrogel before injection. However, beside the dead cells, there should be another influence relating to the shearing process, because the cell proliferation seems to be weakened during the cultural days. After injection, though proliferation could be observed, the cell density on the 7th day did not show much distinct increasing compared with the original hydrogels without injection, implying that the shearing stress might more or less weaken cell vitality.

3.5. Cell counting and analysis

Fig. 4 shows the quantitatively statistics analysis for above-mentioned proliferation. After 7 days' culture in the soft, medium and stiff hydrogels prior to injection (Fig. 4A), the cell number increased 78%, 106% and 145%, respectively. After injection (Fig. 4B), the cell number increased 70%, 88% and 110%, respectively. These values showed clear decrease compared with that of the original groups, where the cells did not suffer the shearing process. Anyway, a positive correlation between the cell proliferation rate and the hydrogel stiffness could be regulated. In addition, the statistical analysis in Fig. 4B revealed there is no significant difference (t-test: $P > 0.05$) between the medium group and the control group. This was well agreed with afore mentioned pretesting in Fig. 4A. But, the

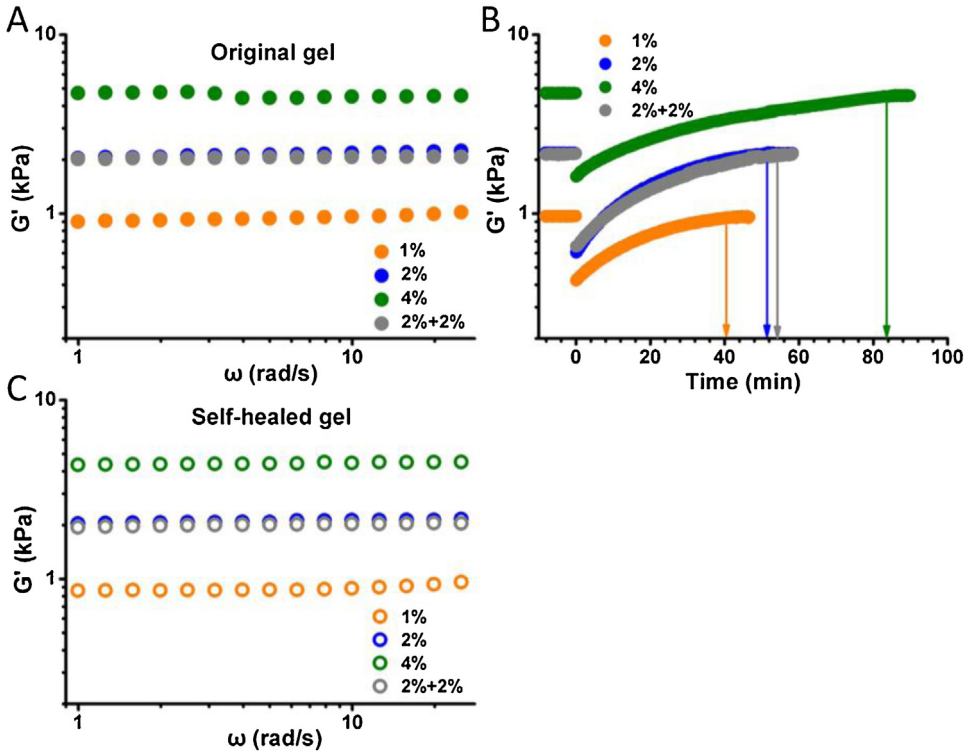

Fig. 1. Storage moduli (G') of the series of hydrogels with different wt% DF-PEG (orange: 1%; blue: 2%; green: 4%; gray: 2% DF-PEG and 2% PEG). (A) Before injection. (B) The self-healing process after injection. (C) Self-healed hydrogels after injection.(For interpretation of the references to colour in this figure legend, the reader is referred to the web version of this article.)

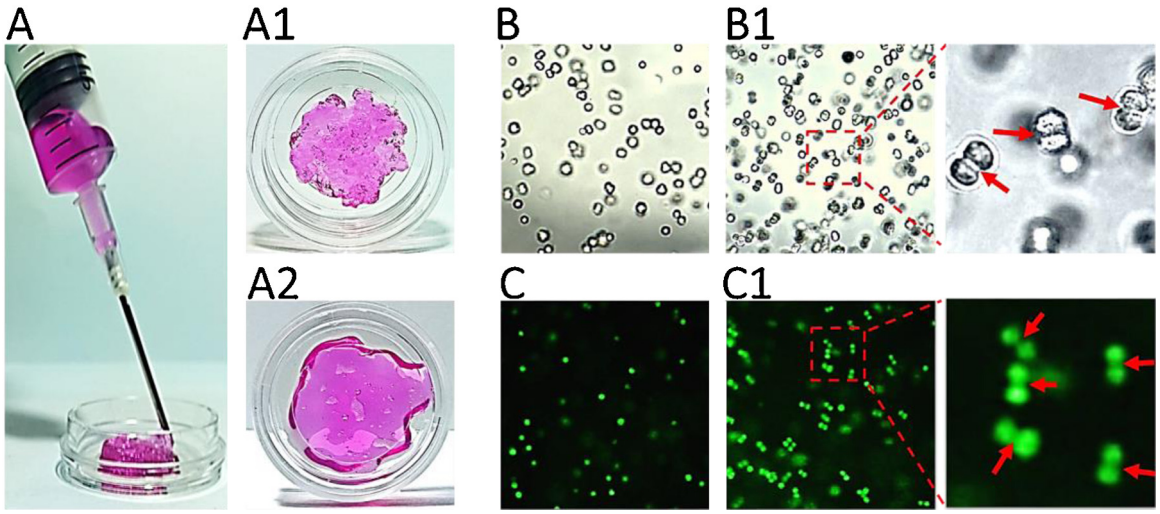

Fig. 2. (A) Injection and self-healing of the cell-embedded CP hydrogel: (A1) Squished CP hydrogel pieces; and (A2) self-healed integrated hydrogel. (B) Optical microscopy and (C) Fluorescent images of the embedded cells: (B, C) on the 1st day; and (B1, C1) on the 7th day.

significant differences (t-test: $P < 0.05$) for the cell numbers among the three experimental groups were only observed on and after the 5th day (Fig. 4B). We noticed that cell numbers in the hydrogels did not show statistical difference on the 3rd day after injection. It might be contributed to two reasons. Firstly, the injection might cut down different numbers of cells, leading to the delay of the statistical difference among different groups. Secondly, cells in stiff hydrogel would suffer higher shearing stress during the injecting process, which might affect the cell vitality.

To demonstrate this hypothesis, all the cell numbers of the encapsulated cells before and after injection were recorded following appointed periods (Fig. 5). It is a critical perspective of cell conditions [39]. It can be easily noticed that the proliferation in the soft hydrogel did not change a lot after injection (rectangle in Fig. 5A). However, the proliferation declined more obviously in stiff hydrogel (rectangle in Fig. 5C). It confirmed that higher modulus could cause higher shearing stress during injection and thus leading to higher cell death or lower cell activity.

To quantitatively evaluate the influence of injection, we compared the slope of the cell proliferation before and after injection, corresponding to K_0 and K_1, respectively. On the 7th day, the cells that did not suffer injection were estimated to touching the plateau because of the capacity limitation; and for the 1st day of the injected cells, they were also estimated to undergo the complicacy caused

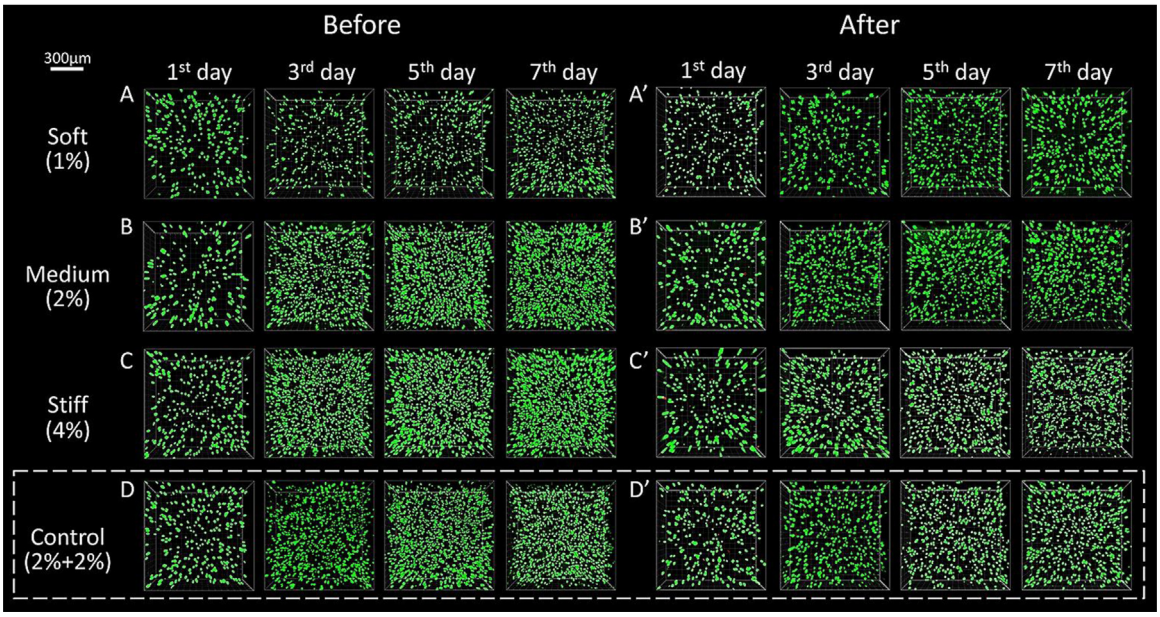

Fig. 3. 3D confocal images of L929 cells embedded in a series of hydrogels with different moduli at denoted cultural times, before (A, B, C, D) and after (A', B', C', D') injection.

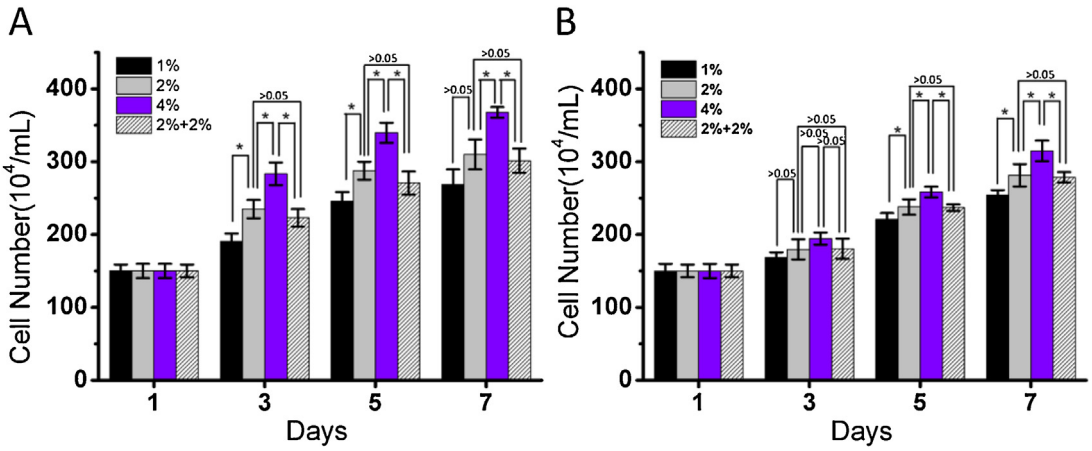

Fig. 4. Cell counting of L929 cells embedded in a series of hydrogels with different modulus at denoted time before (A) and after (B) injection. Data represent mean ± SD (n = 3, *: $p < 0.05$).

Table 1
The slopes[a] of the embedded cells' proliferation.

Samples	K_0	K_1	$(K_0-K_1)/K_0$
1%	24.0	21.5	10.4%
2%	34.4	25.5	25.9%
4%	47.4	30.1	36.5%
2%+2%	30.2	24.5	18.9%

[a] K_0: without receiving injection; K_1: after injection.

by the injection procedure. Therefore, both of them were eliminated from the slope calculation. Through using three points fitting in Fig. 5, slopes were obtained to compare the potential influence of the injecting operation. Table 1 reveals that the hydrogels with higher modulus would affect the proliferation rate more, where decreasing amplitudes from 10.4% to 25.9% and further to 36.5% are displayed according to the sequence of the increased stiffness of those hydrogels. It should be emphasized that this slope is related to cell vitality rather than numbers of dead cells. As a data reference, this is a helpful insight for evaluating the squeezing influence between gel strength and cell proliferation for this injectable hydrogel. Moreover, this data analysis has a potential to act as a guideline for practical cell therapy.

4. Conclusions

A series of chitosan-based hydrogels with different storage moduli were prepared by verifying the amount of the cross-linker (DF-PEG). A significant positive correlation between the proliferation rate of the embedded cells and the modulus of the hydrogels was discovered in the experimental test range, indicating a facile way to control cell proliferation in the hydrogel without extra-added growth factor. It is noted that after injection, the cells have very high viability and keep high proliferation rate in CP hydrogel, suggesting this injectable self-healing hydrogel could not only deliver the implanted cells to the desired spot, but also accelerate the curing by allowing the encapsulated cells to proliferate in situ. Therefore, the CP hydrogel is an ideal candidate to incubate functional cells or stem cells for cell therapy although the balance between positive factor of stiffness and negative factor of shearing force should be considered. In addition, we hope that CP hydrogel

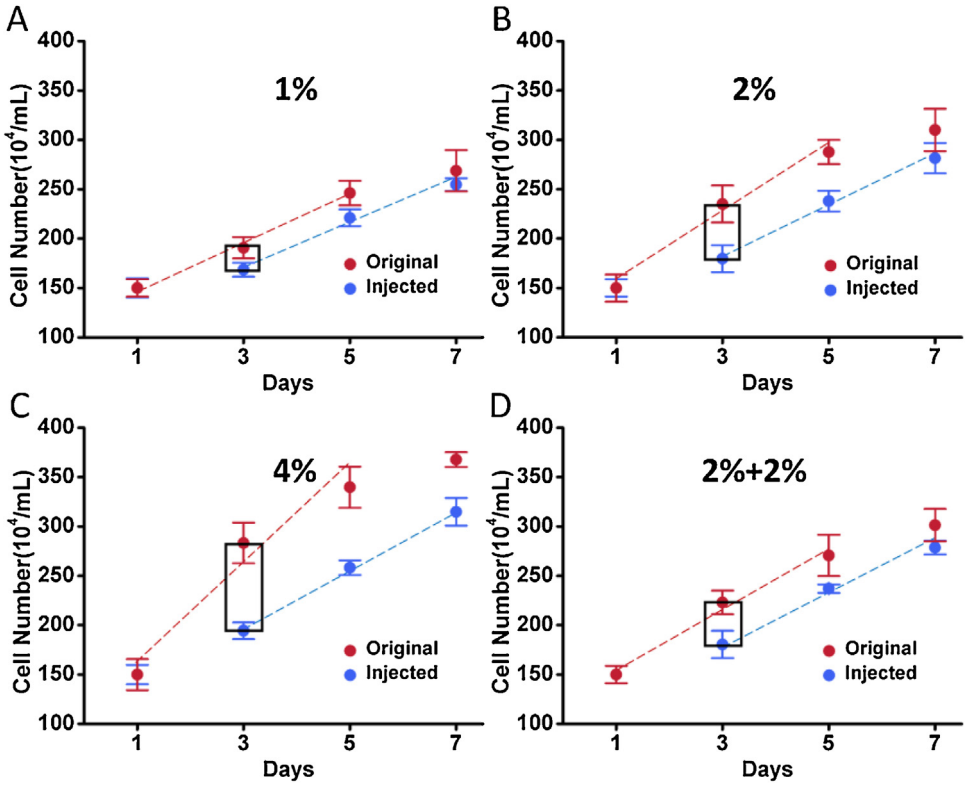

Fig. 5. Quantitation of cell numbers in the original hydrogel (red points) and after injection (blue points). (A) Soft (1%); (B) Medium (2%); (C) Stiff (4%); (D) Control (2%+2%). Linear fittings were displayed with dash lines. Differences of proliferation were remarked with outlined rectangles. (For interpretation of the references to colour in this figure legend, the reader is referred to the web version of this article.)

might broaden the biomedical usage for chemically cross-linked self-healing hydrogels in areas like cell delivery.

Acknowledgments

The authors thank the National Natural Science Foundation of China (21134004, 21574008, and 51302010), the Fundamental Research Funds for Central Universities of China (YS1407), and the BUCT Fund for Disciplines Construction and Development (XK1538) for their funding support. Confocal image was acquired by a Zeiss710-3 channel confocal microscope from center of biomedical analysis Tsinghua University.

Appendix A. Supplementary data

Supplementary data associated with this article can be found, in the online version, at http://dx.doi.org/10.1016/j.colsurfb.2016.10.021.

References

[1] F.H. Gage, Nature 392 (1998) 18.
[2] L.V. Bahr, I. Batsis, G. Moll, M. Hägg, A. Szakos, B. Sundberg, M. Uzunel, O. Ringden, K.L. Blanc, Stem. Cells 30 (2012) 1575.
[3] D.J. Prockop, Mol. Ther. 17 (2009) 939.
[4] J.A.M. Steele, J.-P. Hallé, D. Poncelet, R.J. Neufeld, Adv. Drug. Deliver. Rev. 67 (2014) 74.
[5] G. Orive, R.M. Hernandez, A.R. Gsacon, R. Calafiore, T.M.S. Chang, P.D. Vos, G. Hortelano, D. Hunkeler, I. Lacik, A.M.J. Shapiro, J.L. Pedraz, Nat. Med. 9 (2003) 104.
[6] M.J. Cheng, Y. Wang, L.L. Yu, H.J. Su, W.D. Han, Z.F. Lin, J.S. Li, H.J. Hao, C. Tong, X.L. Li, F. Shi, Adv. Funct. Mater. 25 (2015) 6851.
[7] C. Giordano, D. Albani, A. Gloria, M. Tunesi, S. Batelli, T. Russo, G. Forloni, L. Ambrosio, A. Cigada, Int. J. Artif. Organs. 32 (2009) 836.
[8] C. Giordano, D. Albani, A. Gloria, M. Tunesi, S. Rodilossi, T. Russo, G. Forloni, L. Ambrosio, A. Cigada, Int. J. Artif. Organs. 34 (2011) 1115.
[9] S. Reitmaier, A. Shirazi-Adl, M. Bashkuev, H.J. Wilke, A. Gloria, H. Schmidt, J. R. Soc. Interface. 9 (2012) 1869.
[10] R. Tsaryka, A. Gloriab, T. Russob, L. Anspacha, R.D. Santisb, S. Ghanaati, R.E. Ungera, L. Ambrosiob, C.J. Kirkpatricka, Acta Biomater. 20 (2015) 10.
[11] B.A. Aguado, W. Mulyasasmita, J. Su, K.J. Lampe, S.C. Heilshorn, Tissue Eng. Part. A. 18 (2012) 806.
[12] K.T. Nguyen, J.L. West, Biomaterials 23 (2002) 4307.
[13] L. Yu, J.D. Ding, Chem. Soc. Rev. 37 (2008) 1473.
[14] J.A. Burdick, K.S. Anseth, Biomaterials 23 (2002) 4315.
[15] C.Q. Yan, M.E. Mackay, K. Czymmek, R.P. Nagarkar, J.P. Schneider, D.J. Pochan, Langmuir 28 (2012) 6076.
[16] L. Klouda, Eur. J. Pharm. Biopharm. 97 (2015) 338.
[17] L. Klouda, A.G. Mikos, Eur. J. Pharm. Biopharm. 68 (2008) 34.
[18] H.P. Tan, C.R. Chu, K.A. Payne, K.G. Marra, Biomaterials 30 (2009) 2499.
[19] B. Balakrishnan, A. Jayakrishnan, Biomaterials 26 (2005) 3941.
[20] E. Ruel-Gariepy, J.-C. Leroux, Eur. J. Pharm. Biopharm. 58 (2004) 409.
[21] X.K. Ren, Y.K. Feng, J.T. Guo, H.X. Wang, Q. Li, J. Yang, X.F. Hao, J. Lv, N. Ma, W.Z. Li, Chem. Soc. Rev. 44 (2015) 5680.
[22] J. Zhang, Y. Li, Drug. Discov. Today. 19 (2014) 579.
[23] Y.L. Zhang, L. Tao, S.X. Li, Y. Wei, Biomacromolecules 12 (2011) 2894.
[24] Y.L. Zhang, B. Yang, X.Y. Zhang, L.X. Xu, L. Tao, S.X. Li, Y. Wei, Chem. Commun. 48 (2012) 9305.
[25] Y. Jia, J.B. Li, Chem. Rev. 115 (2014) 1597.
[26] O. Ramström, J.M. Lehn, Nat. Rev. Drug. Discov. 1 (2002) 26.
[27] J.M. Lehn, Chem. Soc. Rev. 36 (2007) 151.
[28] S.J. Rowan, S.J. Cantrill, G.R.L. Cousins, J.K.M. Sanders, J.F. Stoddart, Angew. Chem. Int. Edit. 41 (2002) 898.
[29] N.K. Guimard, K.K. Oehlenschlaeger, J.W. Zhou, S. Hilf, F.G. Schmidt, C. Barner-Kowollik, Macromol. Chem. Phys. 213 (2012) 131.
[30] P. Cordier, F. Tournilhac, C. Soulié-Ziakovic, L. Leibler, Nature 451 (2008) 977.
[31] K. Imato, M. Nishihara, T. Kanehara, Y. Amamoto, A. Takahara, H. Otsuka, Angew. Chem. Int. Edit. 51 (2012) 1138.
[32] T.C. Tseng, L. Tao, F.Y. Hsieh, Y. Wei, I.M. Chiu, S.H. Hsu, Adv. Mater. 27 (2015) 3518.
[33] C. Yang, M.W. Tibbitt, L. Basta, K.S. Anseth, Nat. Mater. 13 (2014) 645.
[34] S. Khetan, M. Guvendiren, W.R. Legant, D.M. Cohen, C.S. Chen, J.A. Burdick, Nat. Mater. 12 (2013) 458.
[35] E.A. Phelps, N.O. Enemchukwu, V.F. Fiore, J.C. Sy, N. Murthy, T.A. Sulchek, T.H. Barker, A.J. Garcia, Adv. Mater. 24 (2012) 64.
[36] J.L. Holloway, H. Ma, R. Rai, J.A. Burdick, J. Control. Release 119 (2014) 63.
[37] M. Geerligs, G.W.M. Peters, P.A.J. Ackermans, C.W.J. Oomens, F.P.T. Baaijens, Biorheology 45 (2008) 677.
[38] B. Yang, Y.L. Zhang, X.Y. Zhang, L. Tao, S.X. Li, Y. Wei, Polym. Chem. 3 (2012) 3235.
[39] L. Tan, J.L. Hu, H.H. Huang, J.P. Han, H.W. Hu, Int. J. Biol. Macromol. 79 (2015) 469.